NASA CR-134614
R-9480

FINAL REPORT

ANALYSIS OF THE EFFECTS OF BAFFLES ON COMBUSTION INSTABILITY

By

C. L. Oberg
W. H. Evers
M. D. Schuman
A. L. Huebner

Rocketdyne Division
Rockwell International
6633 Canoga Avenue
Canoga Park, California

Prepared for
National Aeronautics and Space Administration
Lewis Research Center

Contract NAS3-11226

Dr. R. J. Priem, Technical Monitor

May 1974

1. Report No.	2. Government Accession No.	3. Recipient's Catalog No.
NASA CR-134614		

4. Title and Subtitle	5. Report Date
ANALYSIS OF THE EFFECTS OF BAFFLES ON COMBUSTION INSTABILITY	May 1974
	6. Performing Organization Code
7. Author(s)	8. Performing Organization Report No.
C. L. Oberg, W. H. Evers, M. D. Schuman, and A. L. Huebner	R-9480
	10. Work Unit No.
9. Performing Organization Name and Address	11. Contract or Grant No.
Rocketdyne Division Rockwell International 6633 Canoga Avenue Canoga Park, CA 91304	NAS3-11226
	13. Type of Report and Period Covered
12. Sponsoring Agency Name and Address	Final Report
National Aeronautics and Space Administration Washington, D.C. 20546	14. Sponsoring Agency Code

15. Supplementary Notes

NASA Technical Monitor, Dr. R. J. Priem
NASA-Lewis Research Center
21000 Brookpark Road, Cleveland, OHIO 44135

16. Abstract

An analytical model has been developed for predicting the effects of baffles on combustion instability. This model has been developed by coupling an acoustic analysis of the wave motion within baffled chambers with a model for the oscillatory combustion response of a propellant droplet developed by Heidmann. A computer program was developed for numerical solution of the resultant coupled equations. However, calculations with the model showed that it did not properly predict the experimentally observed variation of stability with increasing baffle length. In fact, the model predicted a worsening of stability with increasing baffle length rather than improving as found experimentally. Diagnostic calculations were made to determine the reasons for the improper prediction. These calculations showed that the chosen method of representing the combustion response was a very poor approximation. At the end of the program, attempts were made to minimize this effect but the model still improperly predicts the stability trends. Therefore, it is recommended that additional analysis be done with an improved approximation.

17. Key Words (Suggested by Author(s))	18. Distribution Statement
Combustion Instability Baffles Instability Suppression	Publicly Available

19. Security Classif. (of this report)	20. Security Classif. (of this page)	21. No. of Pages	22. Price*
UNCLASSIFIED	UNCLASSIFIED	36 & v	

*For sale by the National Technical Information Service, Springfield, Virginia 22151

NOMENCLATURE

c	=	sound velocity, in./sec
D	=	droplet diameter, in.
$G(\vec{r}\|\vec{r}_0)$	=	Green's function
I_{cn}	=	imaginary component at harmonic response factor for n^{th} term, defined by Eq. 14
Im ( )	=	imaginary part of following quantity
i	=	$(-1)^{\frac{1}{2}}$
k	=	complex wave number (complex angular frequency divided by sound velocity) $in.^{-1}$
$k^{(1)}$	=	k for first transverse mode
$k^{(2)}$	=	k for second transverse mode
ℓ	=	baffle length, inches
$\bar{M}$	=	steady flow Mach number
P'	=	oscillatory pressure divided by time averaged pressure
P_n	=	Fourier amplitude coefficient for n^{th} pressure term, Eq. 18
R_{cn}	=	Real component of harmonic response factors for n^{th} term, defined by Eq. 13
Re ( )	=	real part of following quantity
$\mathscr{R}_{cn}$	=	complex harmonic response factors, Eq. 16
$\vec{r}$	=	position vector, inches
S	=	surface area, sq in.
t	=	time, sec
U	=	magnitude of velocity difference between the gas and droplet, in./sec

u_n = Fourier amplitude coefficient for n^{th} velocity term, Eq. 19

u_t = transverse velocity difference between the gas and droplet, in./sec

$\Delta\bar{V}$ = time averaged velocity difference between the gas and liquid

W = burning rate divided by time averaged burning rate

w = burning rate, lbm/sec

β_{2L1} = specific acoustic admittance at injector face for first transverse mode

β_{2L2} = specific acoustic admittance at injector face for second transverse mode

γ = ratio of heat capacities, constant pressure to constant volume

$\eta^{(i)}$ = i^{th} approximation for oscillatory pressure distribution, $lbf/in.^2$

θ_n = phase angle between pressure and velocity, Eq. 19, for n^{th} mode

μ = index referring to μ^{th} compartment

ξ = pressure gradient, Eq. 5, $lbf/in.^3$

ϕ_n = phase angle between terms in pressure expansion, Eq. 18

ϕ_2 = phase angle between first and second pressure harmonics

SUBSCRIPTS

a = refers to main chamber

b = refers to baffle compartments

n = refers to n^{th} harmonic

0 = refers to source coordinates for Green's functions

0L1 = refers to nozzle end condition, first harmonic

2L1 = refers to injector end condition, first harmonic

2L2 = refers to injector end condition, second harmonic

SUPERSCRIPTS

— (over bar) = denotes time averaged value

1 = denotes first harmonic quantity

2 = denotes second harmonic quantity

SUMMARY

An analytical model has been developed to predict the effects of baffles on combustion instability. This model has been developed by coupling an acoustic analysis of the wave motion within baffled chambers (developed during earlier work under this contract) with a model for the oscillatory combustion response of a propellant droplet developed by Heidmann, the response factor model. The response factor model includes a significant contribution from the first harmonic of the fundamental mode of oscillation, which could be calculated from a nonlinear, multiorder perturbation analysis of the wave motion. For this program, the spatial distribution of pressure and velocity for the harmonic contribution were assumed to be equal to those given by the linear acoustic analysis for the harmonic mode.

A computer program was developed for numerical solution of the coupled equations. After this program was thoroughly checked out, a series of calculations was made to investigate the variation of predicted stability with variations in model parameters. This investigation showed that the model as developed did not properly predict the variation of stability with increasing baffle length. The model predicted a worsening of stability with increasing baffle length rather than improving as found experimentally. Therefore, diagnostic calculations were performed to determine the reasons for the improper prediction.

The diagnostic calculations showed that the spatial average injector face boundary condition used to represent the combustion response was a very poor

approximation. The boundary condition varied widely with position. At the end of the program, initial attempts were made to minimize this effect by analysis of cases for more than one baffle, but the model still improperly predicts the stability trends. Therefore, it is recommended that additional analysis be done with an improved approximation to the spatially varying boundary condition. Results from this recommended analysis should allow an adequate assessment of the effectiveness of the general analytical formulation to be made and will allow the best direction for future analysis to be determined.

INTRODUCTION

This report outlines results obtained under NASA Contract NAS3-11226 during the period from April 1971 to March 1974. The report is being prepared and submitted in memorandum form because the available contract funds were intentionally spent essentially completely on attempts to solve technical problems encountered during the program.

The purpose of the program described herein was to develop suitable analytical models to describe the wave motion within, and combustion stability of, baffled combustion chambers. Such models are needed to aid the analysis and design of baffled combustion chambers. During earlier work under this contract, analytical methods were developed to analyze the wave motion in baffled chambers without considering combustion effects. Results from this earlier work are described in Ref. 1 and 2. The effects of combustion were largely ignored during this earlier work except to allow for a gain-type admittance boundary condition. Results from calculations with this admittance-type boundary condition showed a physically unsatisfactory result, increasing baffle length worsened the predicted stability. Because this result is contrary to known stability behavior, it was concluded that the simple pressure coupling described by the model formulation was inadequate and some means of including velocity coupling effects was necessary. Consequently, the more recent work has been directed toward including a better representation of the combustion effects.

Basically the approach taken has been to couple the previously developed acoustic analysis of the wave motion with an analytical representation of the combustion response to an oscillatory flow field, the latter having been developed by M. F. Heidmann of NASA-Lewis (Ref. 3). Several important assumptions were required to allow the coupled model to be constructed. That model has been developed and calculations were made for a number of conditions. However, results from these calculations also show the physically unacceptable result that the predicted stability worsens with increasing baffle length. Therefore, the subsequent technical effort has been directed toward determining the reasons for the unacceptable predicted behavior and attempting to eliminate deficiencies. Satisfactory stability predictions had not been obtained from the coupled model upon completion of the technical effort.

ANALYTICAL APPROACH

A coupled analytical model was developed by combining the acoustic analysis of the wave motion with the Heidmann response factor model. The response factor was used to specify a boundary condition for the acoustic calculation, through an approximate interrelationship. The acoustic calculation was used to specify the oscillatory pressure and velocity environment needed for the response factor calculation. A multidimensional root-finding technique was developed to solve the coupled equations.

ANALYSIS OF WAVE MOTION

The methods of analysis being used to describe the wave motion in the baffled chamber are described in Ref. 1 and 2. The analysis concerns approximate solution of the wave equation, which simply represents a composite of the linearized fluid dynamic equations obtained through the assumption of small variations from the mean (time average) value and neglecting dissipative effects.

Solution of the wave equation for a baffled chamber is complicated by the fact that the standard separation-of-variables technique cannot be used because of the boundary shape. Consequently, the wave equation and boundary conditions have been rewritten as an integral equation which, in turn, has been solved by a combined variational and iterational method, as suggested by Morse (Ref. 4, pg 1039) for similar problems. This approach was found to work very well and has been applied to both two-dimensional and cylindrical

baffled chambers. The effects of combustion driving and nozzle losses have been simulated to some extent through incorporation of gain/loss-type boundary conditions.

The wave equation and accompanying boundary conditions were converted to an integral equation through the use of Green's functions, as described by Morse (Ref. 5, pg. 321).

The Helmholtz equation (which is the wave equation for a harmonic time dependence), i.e.,

$$\nabla^2 p + k^2 p = 0 \tag{1}$$

may be rewritten as

$$p(\vec{r}) = \int_S G(\vec{r}|\vec{r}_o)\, \vec{N} \cdot \vec{\nabla}_o p(\vec{r}_o) dS_o \tag{2}$$

where $G(\vec{r}|\vec{r}_o)$ is a Green's function, which satisfies the same boundary conditions as the pressure (p), and, also, satisfies the differential equation

$$\nabla^2 G + k^2 G = -\delta(\vec{r}-\vec{r}_o) \tag{3}$$

where $\delta(\vec{r}-\vec{r}_o)$ is a Dirac delta function. Expressions for the Green's function may be obtained in several ways, such as described by Morse (Ref. 4, pp 791 to 834).

The integral expression for pressure is used with separate Green's functions written for each baffle compartment and also for the main chamber. Each of these Green's functions is zero outside of the compartment to which it applies. However, the oscillatory pressure and normal component of velocity must be continuous across the conceptual interface between each region. Therefore, at this interface,

$$p_a(\vec{r}_s) = \int_S G_a(\vec{r}_s|\vec{r}_o)\xi(\vec{r}_o)dS_o = -\int_S G_{b_\mu}(\vec{r}_s|\vec{r}_o)\xi(\vec{r}_o)dS_o = p_{b_\mu}(\vec{r}_s) \tag{4}$$

where $G_a(\vec{r}|\vec{r}_o)$ is the Green's function for the main chamber, $G_{b_\mu}(\vec{r}|\vec{r}_o)$ is the Green's function for the μ^{th} baffle compartment, and, to simplify the notation,

$$\xi(\vec{r}_o^s) = \vec{N} \cdot \vec{\nabla}_o \, p_a(\vec{r}_o^s) = -\vec{N} \cdot \vec{\nabla}_o \, p_b(\vec{r}_o^s) \tag{5}$$

Simultaneous solution of Eq. (4) or related equations, to give the allowed frequencies of oscillation and the normal pressure gradient is the pivotal portion of the analysis. Both the Green's functions and ξ depend on frequency. With this information, the oscillatory pressure and velocity at any point in the chamber may be calculated from the integral expression for pressure, Eq. (2), by integration. The velocity components may be obtained from the gradient of the pressure. A variational-iterational technique has been developed to solve Eq. (4) and (6).

This approximate solution technique results from a direct combination of a variational technique, which allows the "best" form of an approximate solution

to be selected, and an iteration technique, which allows an initially selected approximate solution to be systematically improved. The variational procedure results in replacement of Eq. (4) by a characteristic equation; the procedure used is described by Morse and Ingard (Ref. 5, pg 680). Employing the variational function developed by them, with a slight generalization for multiple compartments, a characteristic equation was obtained.

$$\int_{S_t} \xi \int_{S_t} G_a(\vec{r}|\vec{r}_o)\xi dS_o dS + \int_{S_t} \xi \int_{S} G_{b_\mu}(\vec{r}|\vec{r}_o)\xi dS_o dS = 0 \tag{7}$$

Where an approximate normal velocity of the form $u = A\xi$, has been used, the value of the amplitude (A) being optimized by the method. Thus, at this level of approximation, by assuming a reasonable estimate for the normal gradient, ξ, the frequency may be calculated from Eq. (7). Employing the integral expression for pressure (Eq. (2)) Eq. (7) may be rewritten as

$$\int_S \xi(p_a - p_b)dS = 0 \tag{8}$$

If the exact expression for ξ is obtained, then Eq. (8) is satisfied identically because $p_a = p_b$. However, as it has been used, the variational procedure does not indicate how to estimate ξ; rather, it indicates that the best estimate of the allowed frequencies corresponding to a particular estimate of ξ is obtained by satisfying Eq. (8). The iteration procedure is used to obtain an arbitrarily good estimate of ξ. Nonetheless, continuity of pressure at the interface is satisfied only in the average sense

defined by Eq. (8). The iteration procedure has been set up so that an initial estimate of ξ may be improved with iterations such that in the limit $p_a = p_b$.

The iteration procedure consists of assuming a pressure distribution for p_b, calculating the corresponding ξ and then p_a from that ξ (by employing the integral expression for pressure). A new estimate is obtained for p_b by equating it to the newly calculated p_a. All of this is possible because the expressions for p_a, p_b and ξ are expressed as series of orthogonal functions.

If $\eta^{(i)}$ is used to denote the i^{th} approximation to p_b, the characteristic equation may be written as

$$\int_{St} N \cdot \nabla\eta^{(i)} \left\{ \eta^{(i)} - \eta^{(i+1)} \right\} dS = 0 \qquad (9)$$

This procedure leads to series-type algebraic expressions for the characteristic equation and the pressures. These are easily solved by numerical means. By such means, convergence of the iteration scheme has been demonstrated, i.e., p_a does indeed approach p_b with iterations.

RESPONSE FACTOR ANALYSIS

A model was used to represent the propellant combustion which was based on a model developed by M. F. Heidmann (Ref. 3). Heidmann developed a response factor which was intended to represent the rate of oscillatory energy generation from the propellant combustion. This factor was developed from consideration of combustion of a single droplet, assuming vaporization controlled combustion.

A representation of the droplet combustion rate of the form

$$w \alpha \left(\frac{\rho UD}{\mu}\right)^{\frac{1}{2}} \tag{10}$$

was considered. Oscillatory parameters were defined with reference to time-averaged (but not zero amplitude) conditions, i..e,

$$\rho = \overline{\rho}(1 + \rho') \tag{11}$$

A nonlinear in-phase response factor was defined as

$$R_{n\ell} = \frac{\int_0^{2\pi} W'P'd\omega t}{\int_0^{2\pi} (P')^2 \, d\omega t} \tag{12}$$

Heidmann also defined harmonic response factors,

$$R_{cn} = \frac{\int_0^{2\pi} W \, P_n \cos(n\omega t - \phi_n) \, d\omega t}{\int_0^{2\pi} P_n^{\,2} \cos^2(n\omega t - \phi_n) d\omega t} \tag{13}$$

He found the harmonic content of the pressure environment of the droplet to have a very significant effect on the response factor.

For the current program, harmonic response factors were used for the first and second harmonic modes, these being defined by

$$R_{cn} + i\, I_{cn} \equiv \frac{\int_0^{2\pi} W'\, P_n\, d\omega t}{\int_0^{2\pi} \left[\mathrm{Re}\ (P_n)\right]^2\, d\omega t} \tag{14}$$

The oscillatory pressures, velocities and densities to be used in evaluation of these integrals were obtained from the baffled-chamber acoustic calculation. For simplicity, the integrations were performed numerically. Near the end of the program, the Heidmann formulation was extended to account for non-zero oscillatory growth or decay.

COUPLED ANALYSES

The response factor analysis was coupled to the acoustic analysis through an approximate boundary condition. The analysis of McClure and Cantrell (Ref. 6 and 7) was used to aid definition of the interface condition.

Through analysis of the stability of a chamber with steady flow, Cantrell developed a stability relationship which indicates the stability of a chamber with steady flow can be predicted from a no-flow analysis if an artificial boundary condition is used. Cantrell defines a response function for a surface which is similar in form to the Heidmann response factor. Based on this work by Cantrell, an interface condition was chosen as

$$\gamma \overline{M}\, R_{cn} = \beta_n \tag{15}$$

where β is the wall specific acoustic admittance and $\overline{M}$ is the steady flow Mach number. In addition, for simplicity, the response factor was spatially averaged over the cross section so that a spatially uniform admittance could be used.

Because Heidmann had found the effect of wave distortion to be highly significant in determining the response factor, for the current program it was deemed necessary to include wave distortion in some manner for the evaluation of the response factor. However, the analysis of the chamber acoustics was linear and could not predict distortion. Extending the analysis to a multiorder perturbation scheme to predict nonlinearities, such as done by Maslen and Moore (Ref. 8), appeared unreasonable. Therefore, an assumption was made that the distortion would arise from a harmonic mode to the fundamental which would behave spatially as the harmonic (linear) chamber mode as well.

Solution of the coupled analytical modes represents a complicated root finding problem. A procedure was developed for solving these equations which attempted to make use of varying degrees of difficulty of solving different aspects of the problem.

The overall iterative solution procedure comprises a set of sequential iterative solution procedures. The coupled model is used with a four-dimensional Newton-Raphson procedure to calculate the fundamental-mode injector-end admittance (real and imaginary parts), the harmonic mode pressure amplitude (P_{02}) and the phase angle between the fundamental and harmonic modes (ϕ_2). The fundamental mode amplitude (P_{01}) and steady-state axial gas-to-droplet velocity difference ($\Delta\bar{V}$), as well as the chamber configuration, Mach number, γ, etc., are considered parameters in the calculation. The solution procedure occurs as:

1. Choose initial valves for P_{02}, ϕ_2, β_{2L1}, $k^{(1)}$, β_{2L2}

2. Solve acoustic equations (Newtons' method) for $k^{(1)}$ corresponding to β_{2L1}

3. Calculate fundamental mode pressure and velocity distributions P_1, u_1, v_1

4. For $k^{(2)} = 2\ \mathrm{Re}(k^1) + i\ \mathrm{Im}(k^1)$ solve for corresponding harmonic admittance from acoustic equations.

5. Calculate harmonic mode pressure and velocity distributions.

6. Adjust P_{02} and ϕ_2 (through use of Newtons' method) until $\beta_{2L2} = \gamma\bar{M}\, R_{c2}$.

   6a. Calculate local response factors (n = 1 and 2)

$$\mathcal{R}_{cn} = R_{cn} + i\, I_{cn} = \frac{\int_0^{2\pi} W'\, P_n\, d\omega t}{\int_0^{2\pi} \mathrm{Re}\,(P_n)^2\, d\omega t} \tag{16}$$

   6b. Calculate spatially averaged response factors

$$\overline{\mathcal{R}_{cn}} = \frac{\int_S \mathcal{R}_{cn}\, \mathrm{Re}\,(P_n)^2\, dS}{\int_S \mathrm{Re}\,(P_n)^2\, dS} \tag{17}$$

7. Replace β_{2L1} by $\gamma\bar{M}\,\bar{R}_{c1}$

8. Increment P_{02}, ϕ_2 and β_{2L1} and calculate corresponding $\mathcal{R}_{c1}$ and $\mathcal{R}_{c2}$

9. Using four-dimensional Newtons' method, solve for new estimates for P_{02}, ϕ_2 and β_{2L1}; return to step 2 and continue until convergence is achieved on β_{2L1}.

A computer program has been developed which solves the model equations in this manner for the two-dimensional case. This program was originally developed on a Honeywell 440 timesharing computer for a one-baffle case. A timesharing computer was used because of the frequent need for user interaction to successfully solve the equations. Near the end of the effort, the program was converted to an IBM-370 TSO (timesharing) computer when it became desirable to analyze multibaffle cases (the H-440 was prohibitively slow because of the size and number of operations of the program). Calculations have been made for many cases to investigate the predicted behavior.

RESULTS

A substantial portion of the effort on this program was directed toward developing and checking out the necessary computer program to solve the coupled equations. Subsequently, a number of calculations were made to investigate the predicted behavior. These calculations have all been made with $\gamma = 1.2$, $\bar{M} = 1/3$ and generally with nozzle admittance $\beta_n = 0.0 + i\ 0.0$.

The initial calculations were directed toward investigating the effect of baffle length on the predicted stability. The results are summarized below (for a chamber length-to-width ratio of 1, and $P_{01} = 0.2$):

ℓ	$k^{(1)}$	β_{2L1}	P_{02}	ϕ_2/π
0.020	3.2220 + 0.03123i	-0.2536 + 0.3315i	0.13906	-0.36332
0.100	3.2292 + 0.04830i	-0.3908 + 0.3592i	0.139182	-0.30644
0.150	3.2266 + 0.06858i	-0.4399 + 0.3301i	0.121892	-0.27313
0.200	3.2114 + 0.12815i	-0.4403 + 0.2621i	0.108021	-0.32056
0.250	3.1131 + 0.19331i	-0.3295 + 0.1998i	0.061798	-0.37978
0.300	2.8193 + 0.23135i	-0.2144 + 0.0791i	0.018374	-0.41505
0.330	2.6806 + 0.22877i	-0.1924 + 0.0489i	0.010915	-0.45221
0.370	2.5116 + 0.22455i	-0.1785 + 0.0200i	0.005728	-0.50542
0.375	2.4920 + 0.22439i	-0.1778 + 0.0172i	0.005300	-0.51188
0.380	2.4725 + 0.22431i	-0.1773 + 0.0145i	0.004902	-0.51840
0.500	2.0851 + 0.22211i	-0.1812 - 0.0176i	0.000874	-0.67324
0.600	1.8454 + 0.20969i	-0.1854 - 0.0231i	0.000337	-0.83374
0.700	1.6527 + 0.19364i	-0.1871 - 0.0245i	0.000227	-0.96188
0.800	1.4942 + 0.17713i	-0.1879 - 0.0251i	0.000190	-1.02869

Similar calculations were made for $P_{01} = 0.4$. The results from both sets of calculations are shown graphically in Fig. 1 through 3.

The oscillatory growth coefficient, the imaginary part of the eigenvalue, increases to a maximum and then diminishes slightly. This implies a worsening of predicted stability with increasing baffle length until the maximum is reached. Thus, the problem previously encountered with a simple gain-type boundary condition was again encountered. Because of this non-physical result, the computer program and equations were thoroughly checked out but were found correct.

In an effort to better understand the behavior, calculations were made for a very short-length baffle, $\ell/L = 0.02$. The results are summarized below (for L/W = 1.5):

ℓ	$k^{(I)}$	$\beta_{2L1} = \gamma M \bar{R}_{c1}$	P_{01}	P_{02}	ϕ_2/π
0.02	3.2304 + 0.02618i	-0.2586 + 0.4187i	0.15	0.1225	-0.3795
↓	3.2220 + 0.03123i	-0.2536 + 0.3315i	0.20	0.1391	-0.3633
	3.2163 + 0.03597i	-0.2569 + 0.2780i	0.25	0.1536	-0.3480
	3.2123 + 0.04020i	-0.2621 + 0.2379i	0.30	0.1684	-0.3336
	3.2092 + 0.04386i	-0.2668 + 0.2091i	0.35	0.1837	-0.3196
	3.2067 + 0.04708i	-0.2711 + 0.1864i	0.40	0.1994	-0.3065
	3.2031 + 0.05265i	-0.2786 + 0.1518i	0.50	0.2312	-0.2845
	3.1992 + 0.05702i	-0.2798 + 0.1235i	0.60	0.2603	-0.2602
	3.1949 + 0.06031i	-0.2780 + 0.1006i	0.70	0.2863	-0.2525
	3.1912 + 0.06295i	-0.2736 + 0.08092i	0.80	0.3103	-0.2307
	3.1873 + 0.06488i	-0.2667 + 0.06378i	0.90	0.3328	-0.2108

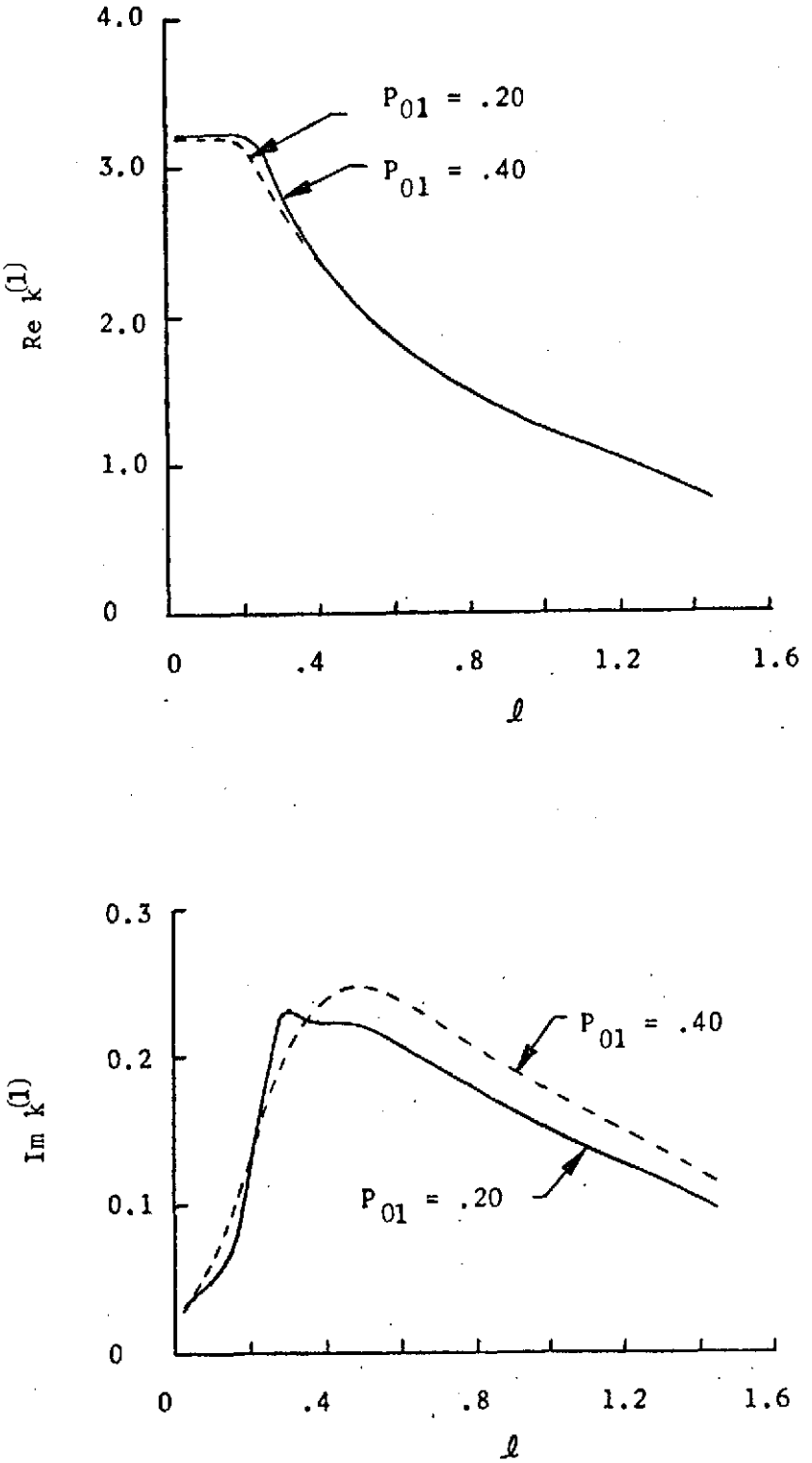

Figure 1. Variation of Frequency (Re $k^{(1)}$) and Growth Coefficient (Im $k^{(1)}$) with Baffle Length (ℓ)

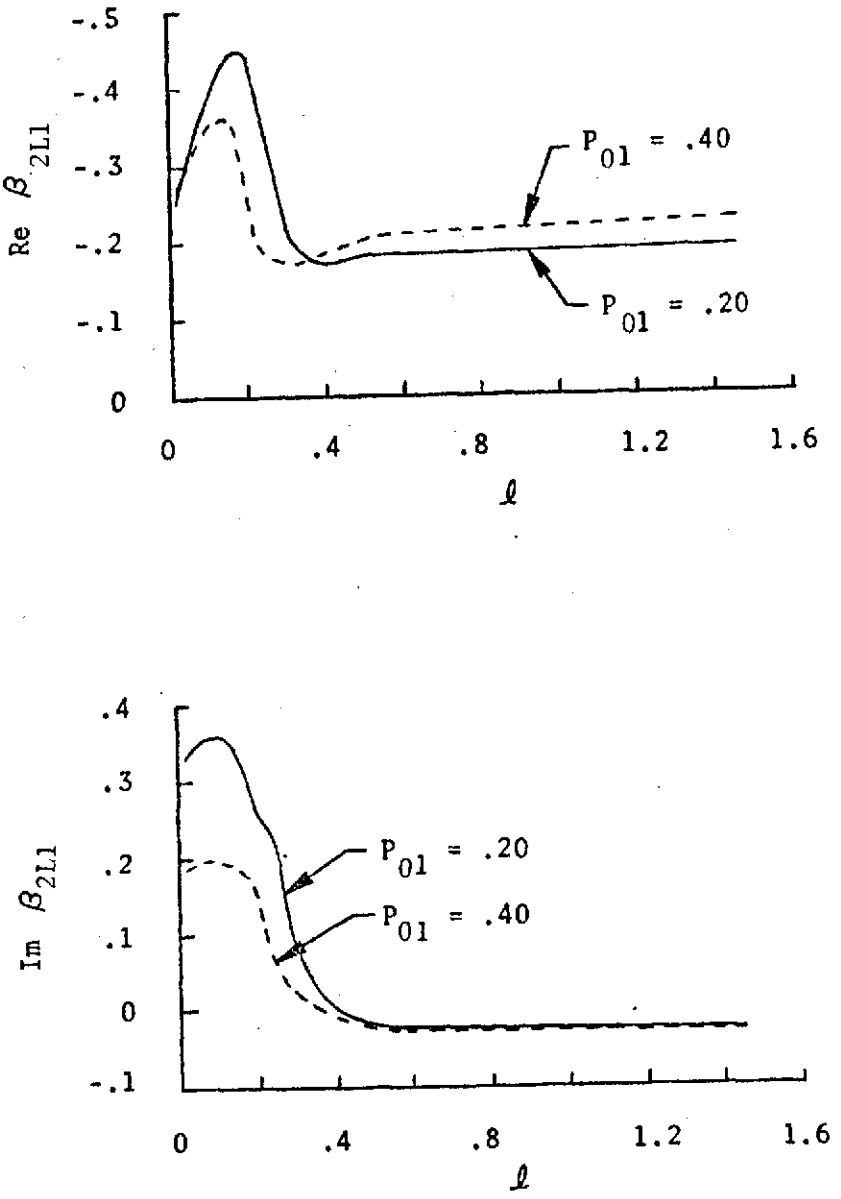

Figure 2. Variation of Fundamental Mode Injector Admittance (β_{2L1}) with Baffle Length (ℓ)

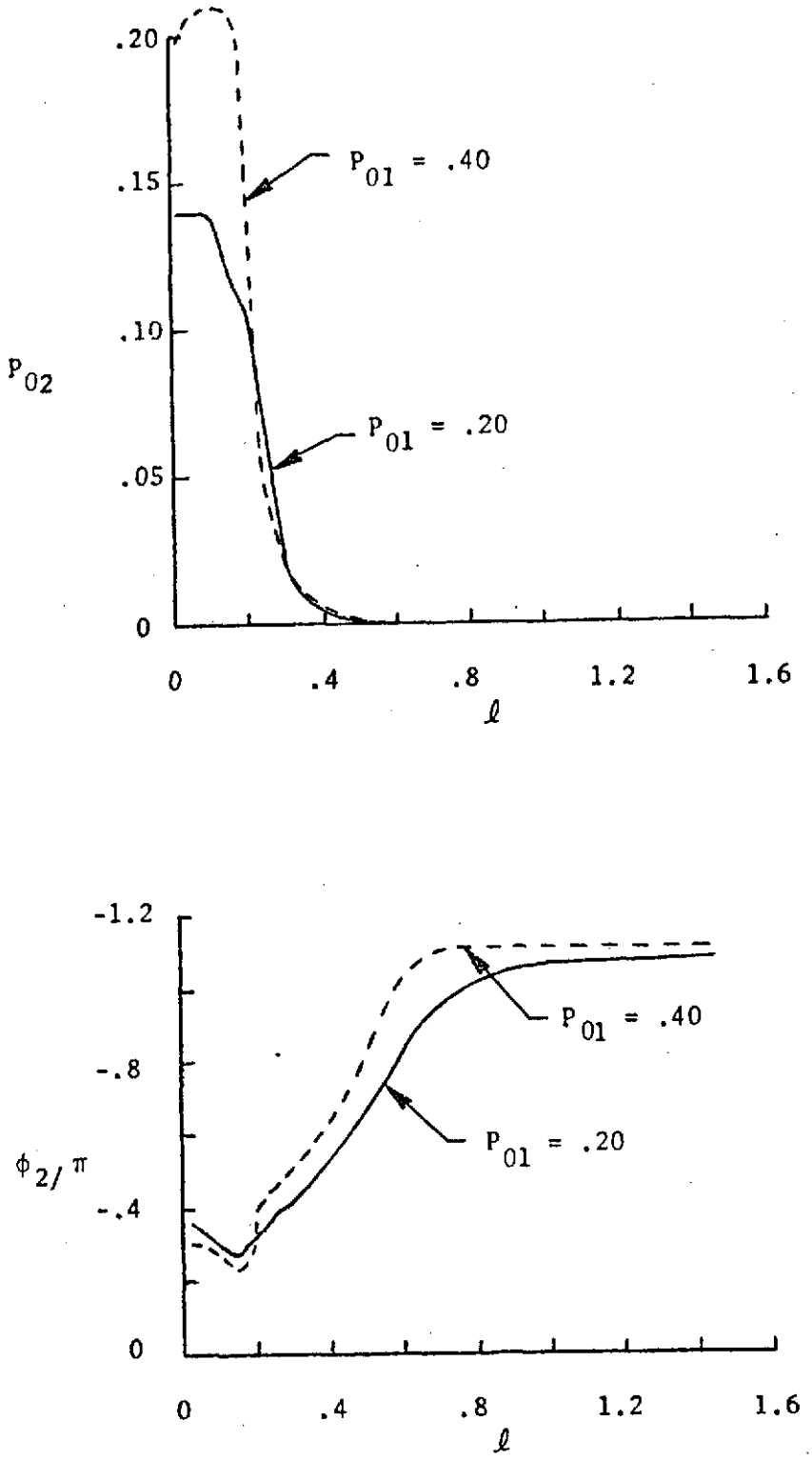

Figure 3. Variation of Second Harmonic Mode Amplitude (P_{02}) and Phase ($\phi_{2/\pi}$) with Baffle Length (ℓ)

The growth coefficient variation with baffle length exhibited by these results is shown in Fig. 4.

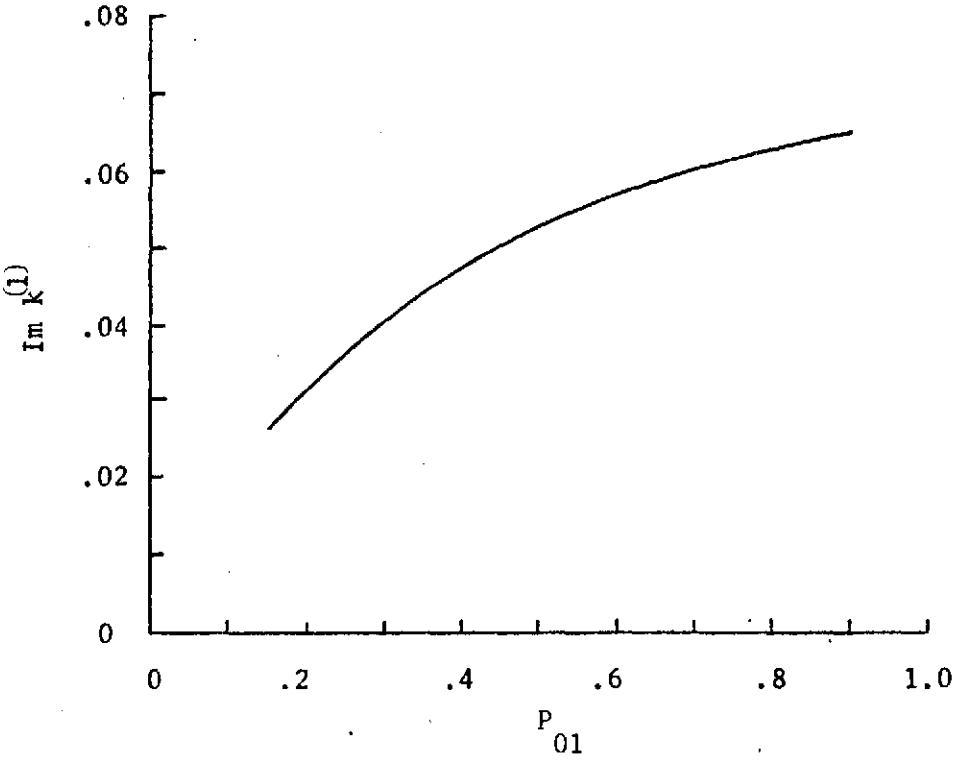

Figure 4. Variation of Growth Coefficient (Im $k^{(1)}$) with Fundamental Mode Amplitude (P_{01})

This behavior appears reasonable and does not indicate an explanation of the nonphysical baffle length effect.

Calculations were also made to investigate the effect of varying the steady-state axial droplet-to-gas velocity difference, $\Delta\bar{V}$. These results are summarized below ($\ell/W = 0.02$, $P_{01} = 0.2$ $L/W = 1.5$).

ℓ	$\overline{\Delta V}$	$k^{(1)}$	$\beta_{2L1} = -M\bar{R}_{c1}$	P_{02}	ϕ_2/π
0.02	0.005	3.2302 + 0.03321i	-0.3102 + 0.3758i	0.1675	-0.3389
↓	0.010	3.2288 + 0.03254i	-0.2969 + 0.3665i	0.1607	-0.3450
	0.020	3.2220 + 0.03123i	-0.2536 + 0.3315i	0.1391	-0.3633
	0.025	3.2188 + 0.03071i	-0.2370 + 0.3133i	0.1288	-0.3753
	0.030	3.2155 + 0.03069i	-0.2244 + 0.2937i	0.1197	-0.3847
	0.035	3.2130 + 0.03132i	-0.2187 + 0.2769i	0.1131	-0.3905
	0.040	3.2112 + 0.03240i	-0.2177 + 0.2623i	0.1085	-0.3924
	0.045	3.2096 + 0.03379i	-0.2198 + 0.2490i	0.1051	-0.3913
	0.050	3.2083 + 0.03541i	-0.2235 + 0.2362i	0.1024	-0.3878
	0.060	3.2056 + 0.03912i	-0.2333 + 0.2114i	0.0983	-0.3787
	0.075	3.2017 + 0.04521i	-0.2473 + 0.1741i	0.0937	-0.3565

Again the behavior appears reasonable and the results did not suggest an explanation for the nonphysical baffle length result.

A series of calculations were then made for a chamber length-to-width ratio of 1.0 and $\Delta\overline{V} = 0.2$. The results are shown below:

ℓ	P_{0I}	$k^{(1)}$	$\beta_{2L1} = -M\bar{R}_{c1}$	P_{02}	ϕ_2/π
0.00	0.10	3.3204 + 0.06544i	-0.3522 + 0.4895i	0.07585	-0.3073
0.05	↓	3.3363 + 0.08148i	-0.4743 + 0.5206i	0.08348	-0.2703
0.15		3.3317 + 0.1443i	-0.6360 + 0.4271i	0.07632	-0.1901
0.25		3.1322 + 0.3258i	-0.4724 + 0.1957i	0.04658	-0.2168
0.35		2.5402 + 0.2129i	-0.1813 + 0.03679i	0.00408	-0.4715
0.50		2.0245 + 0.2004i	-0.1715 - 0.02048i	0.000469	-0.6409
0.00	0.20	3.2885 + 0.08982i	-0.3598 + 0.3109i	0.1092	-0.2600
0.05	↓	3.2948 + 0.1014i	-0.4045 + 0.3197i	0.1134	-0.2413
0.15		3.2764 + 0.1905i	-0.5242 + 0.2278i	0.1160	-0.1392
0.20		3.1857 + 0.2643i	-0.4550 + 0.1612i	0.1038	-0.1702
0.30		2.7483 + 0.2237i	-0.2101 + 0.07423i	0.01695	-0.4184
0.40		2.3454 + 0.2136i	-0.1757 + 0.006862i	0.003622	-0.5384
0.50		2.0298 + 0.2108i	-0.1803 - 0.01645i	0.000907	-0.6584
0.00	0.40	3.2625 + 0.12585i	-0.3942 + 0.1586i	0.1814	-0.1387
0.05	↓	3.2592 + 0.1415i	-0.4111 + 0.1474i	0.1877	-0.1207
0.15		3.1839 + 0.2053i	-0.3852 + 0.1103i	0.2163	-0.1456

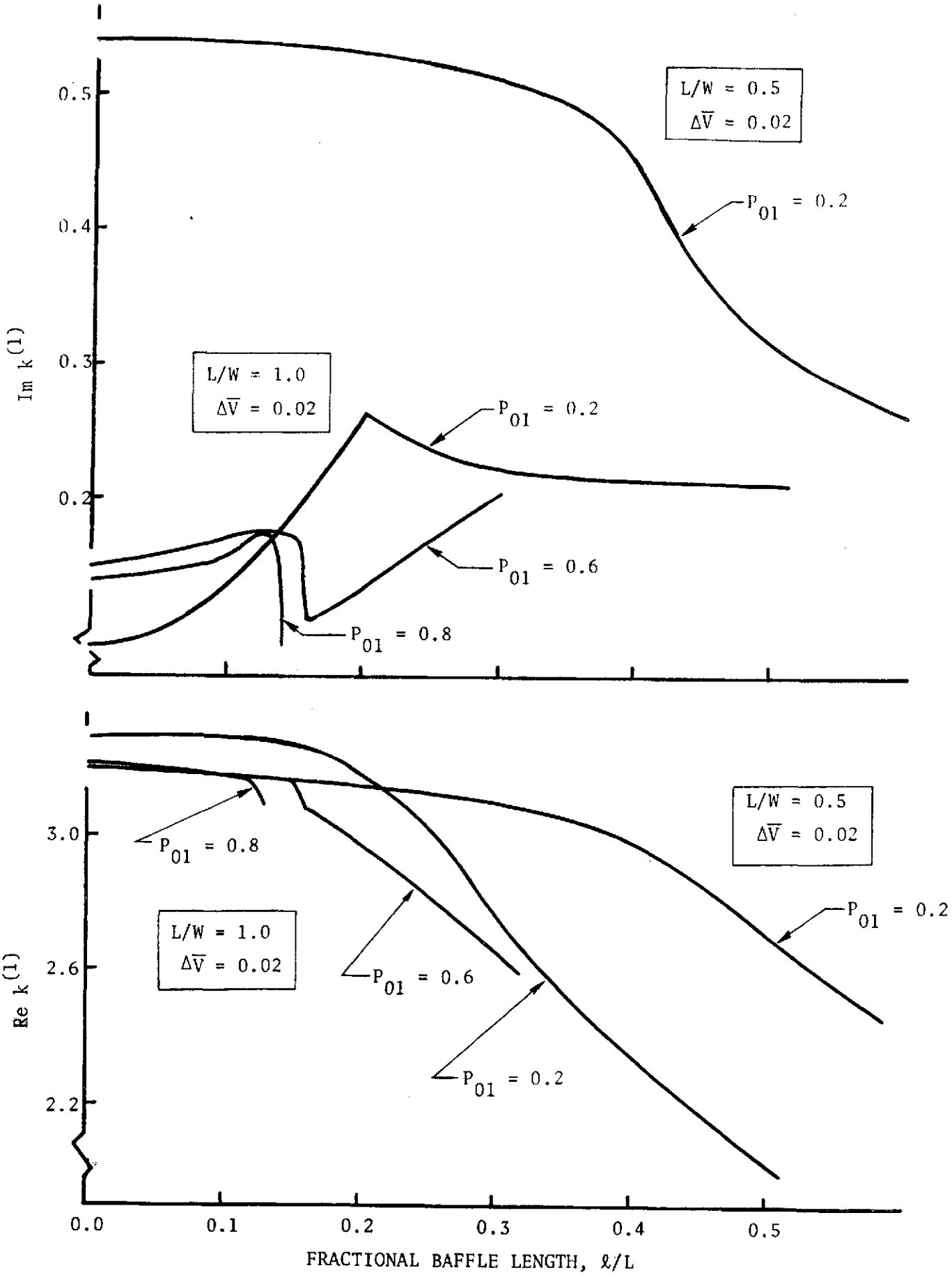

Figure 5. Variation of Fundamental Mode Eigenvalue with Baffle Length

These results exhibit behavior similar to that obtained with L/W = 1.5, i.e., increasing growth coefficient (Im $k^{(1)}$) with increasing baffle length up to a peak value, followed by decreasing values of growth coefficient. However, the sharpness of the peak is more pronounced in the latter case. The eigenvalue results from these calculations are plotted in Fig. 5.

The abrupt changes exhibited by the growth coefficient (Fig. 5) suggested that they corresponded to two different curves, one of which might be associated with an extraneous root obtained from the root-finding process. As a check on this, the calculated baffle compartment and main-chamber pressure profiles were examined at positions on either side of the peak. These profiles were found to agree very closely; therefore, the results correspond to valid solutions to the equations.

The sharp peak exhibited by the growth coefficient curves does not appear reasonable physically and was considered another anomally. Thereafter, extensive diagnostic calculations were made which verified that the computer program correctly executed the desired computations. However, the diagnostic calculations indicated that the anomalous behavior of the growth coefficient with increasing baffle length was the result of one or both of the following: (1) the presence of loops in the acoustic solutions, and (2) poor representation of the local response factor by an average response factor.

The first of these is illustrated in Fig. 6 , which shows an acoustic solution map for the second transverse mode in a two-dimensional unbaffled chamber. For the representative case shown the nozzle admittance is zero and the ratio

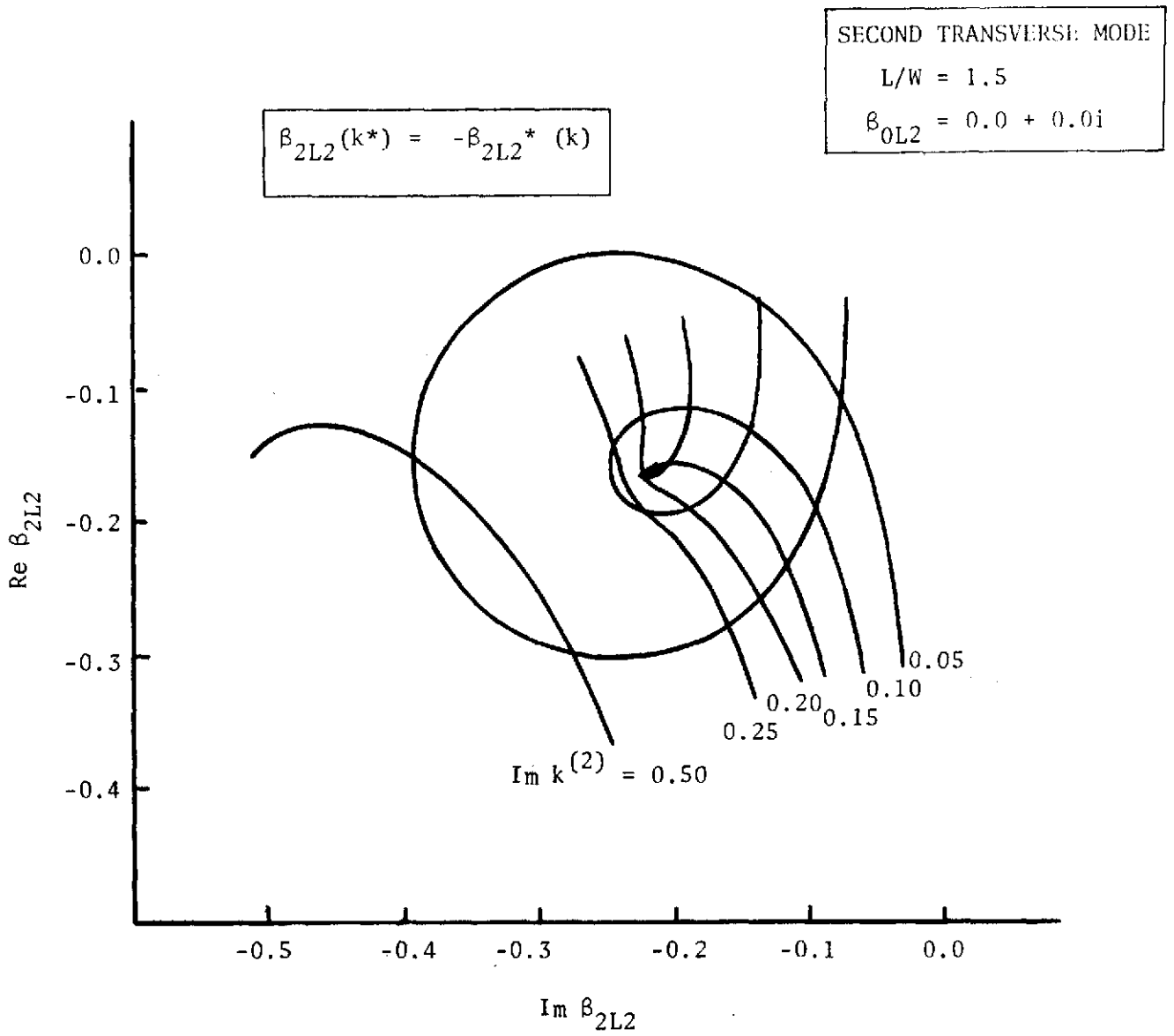

Figure 6. Map of Acoustic Solutions for Second Transverse Mode and One Baffle

of chamber length to chamber width is 1.50. Solution curves are shown for fixed values of the growth coefficient Im $k^{(2)}$. The frequency Re $k^{(2)}$ varies continuously as a single curve is traversed with the loop occurring in the neighborhodd of Re $k^{(2)} = 2\pi$. Consequently, the map shows the value of the injector admittance corresponding to a given eigenvalue ($k^{(2)}$). The loops which appear on some of the solution curves of Fig. 6 are expected to cause both the root-finding process and the solution itself to be very sensitive to the value of the injector admittance. It appears that the regions of this sensitivity agree well with the region for which the anomalous behavior of the growth coefficient occurs.

The discrepancy between the local response factor and its representation by the average response factor is shown on Fig. 7 and 8 for a typical case. Figure 7 shows the real part of the local response factor for the fundamental ($\mathcal{R}_{c1}$) and harmonic ($\mathcal{R}_{c2}$) modes, and the average values ($\bar{\mathcal{R}}_{c1}$, $\bar{\mathcal{R}}_{c2}$) employed in obtaining self-consistent solutions. (The burning rate ($\bar{W}$) is also shown.) Figure 8 shows the corresponding imaginary parts. It is clear from these plots that, for the harmonic mode, the average response factor gives a very poor representation of the local response factor.

Figures 9 and 10 are analogous to Fig. 7 and 8, the only difference being a slightly shorter baffle in the former case. Particularly noteworthy is that the imaginary part of $\mathcal{R}_{c2}$ differs dramatically in the two cases, yet the imaginary part of $\bar{\mathcal{R}}_{c2}$ varies very little between these cases.

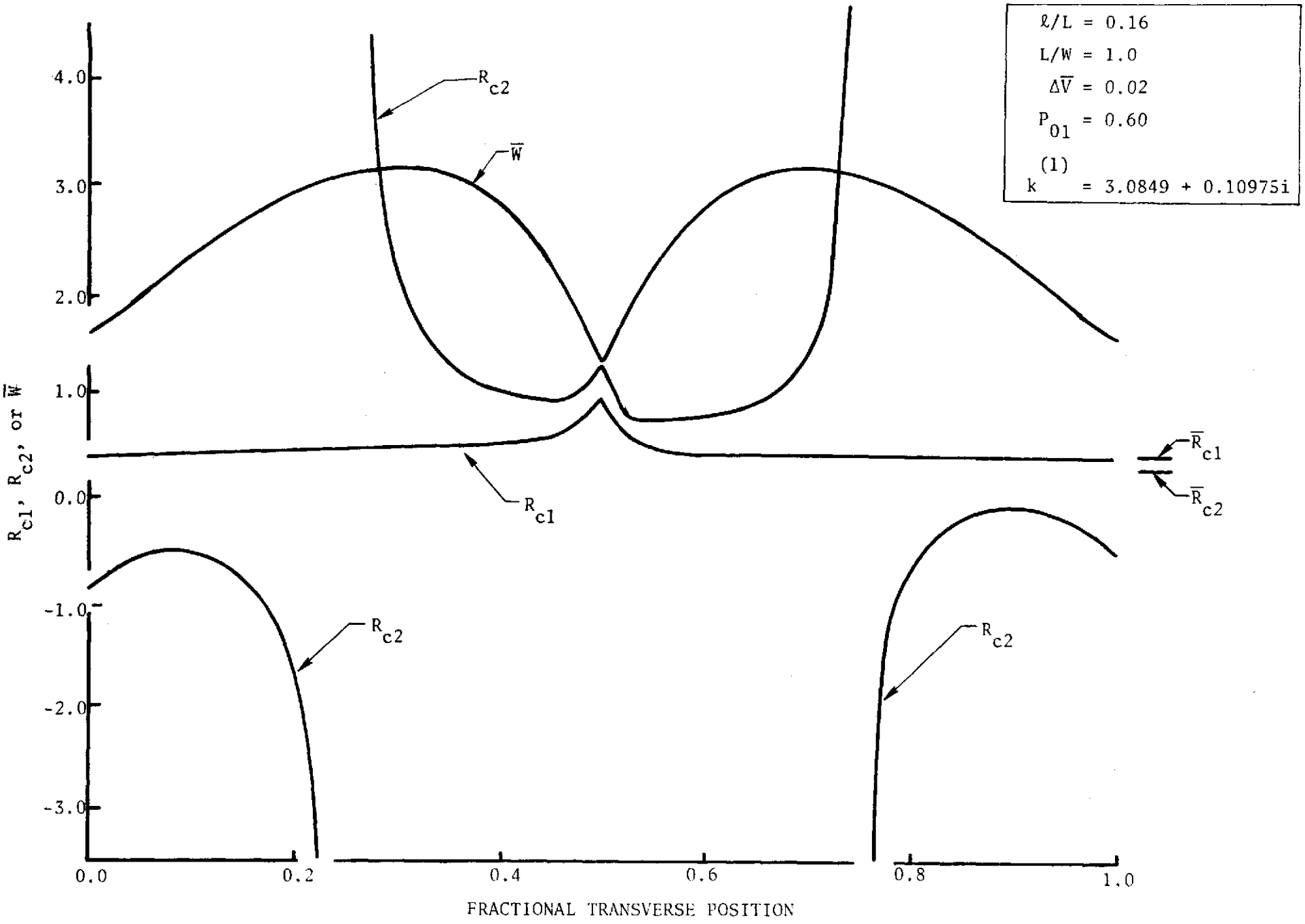

Figure 7. Variation of R_{c1}, R_{c2}, and $\overline{W}$ with Transverse Position, $\ell/L = 0.16$

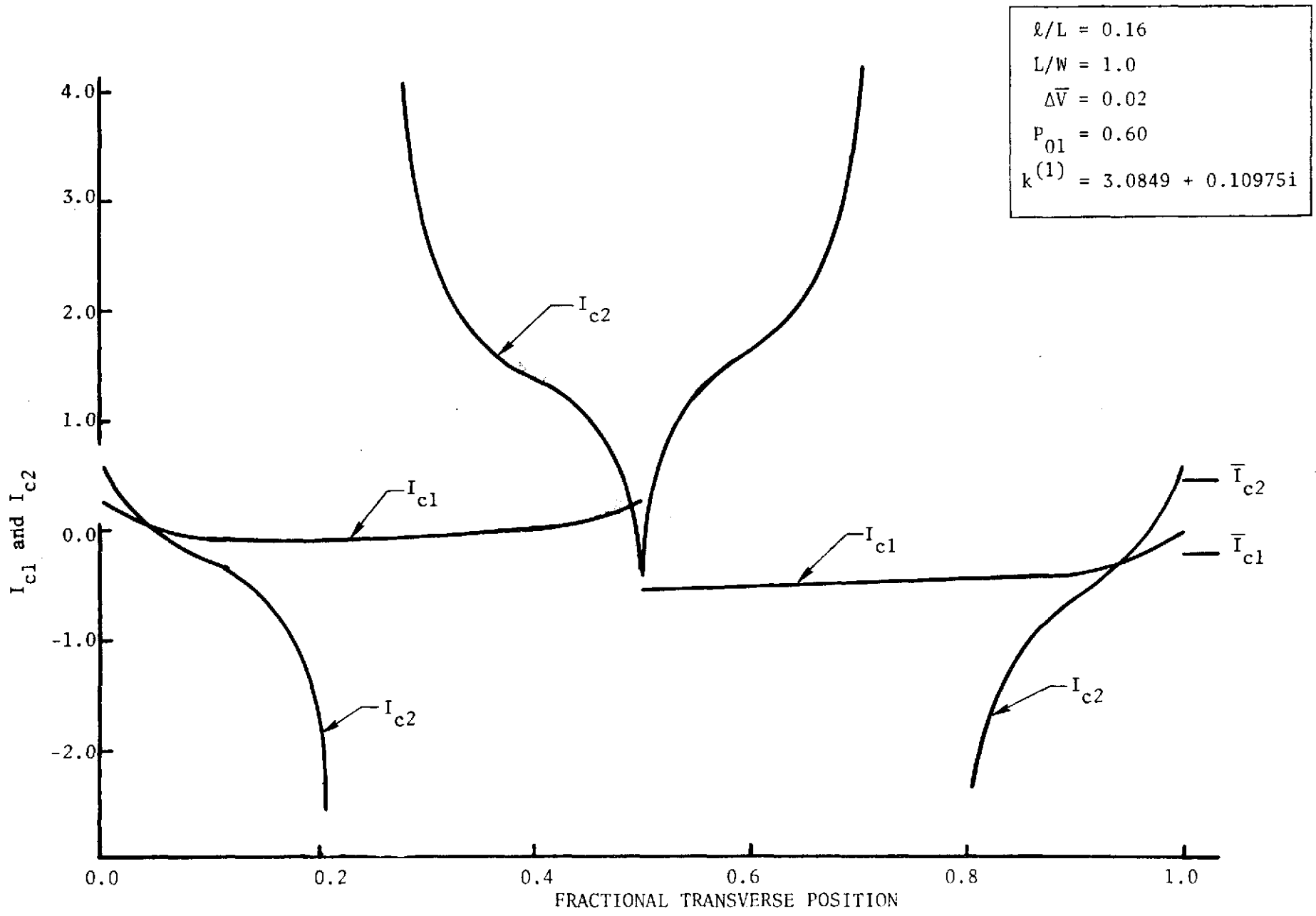

Figure 8. Variation of I_{c1}, I_{c2} with Transverse Position, ℓ/L = 0.16

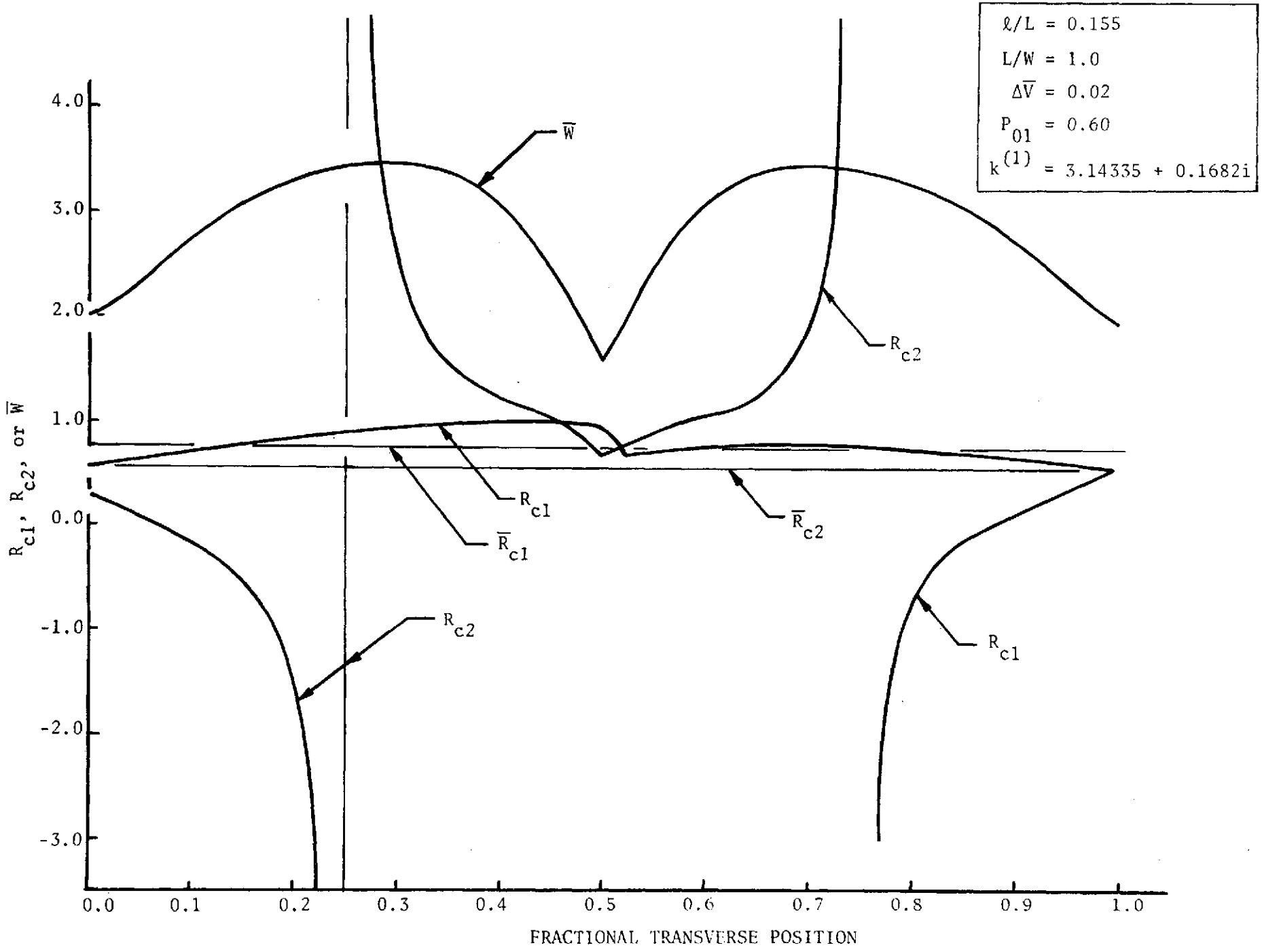

Figure 9. Variation of R_{c1}, R_{c2}, and $\overline{W}$ with Transverse Position, $\ell/L = 0.155$

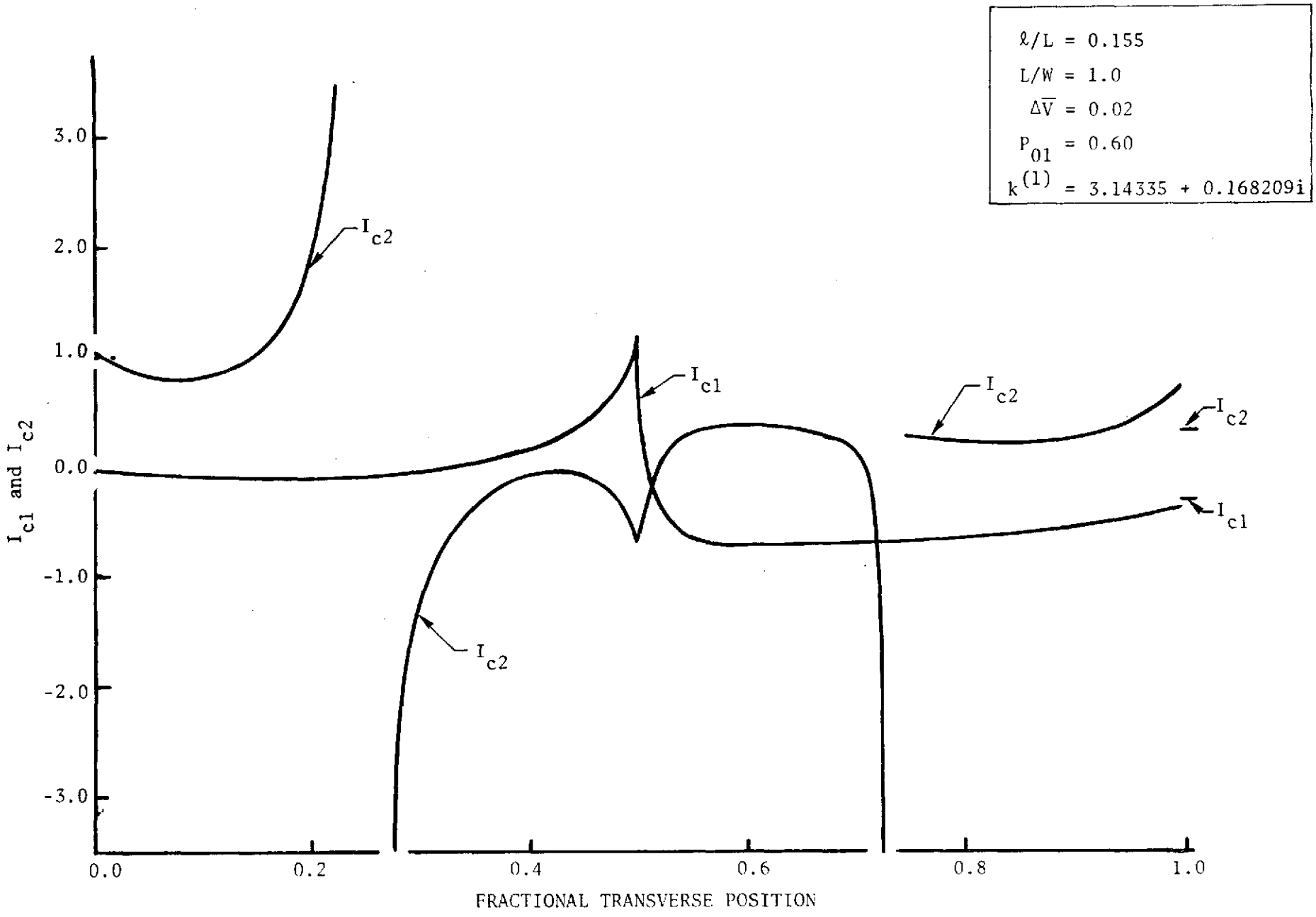

Figure 10. Variation of I_{c1} and I_{c2} with Transverse Position, $\ell/L = 0.155$

As a result of the disparity between local and average response factors it was decided to extend Heidmann's analysis (Ref. 3) to the case of non-zero growth coefficient. The resulting equations are summarized as follows:

$$p' = \sum_{n=1}^{\infty} p_n e^{\alpha t} \cos (n\omega t - \phi_n) \qquad (18)$$

$$k_n = n\omega + i\alpha$$

$$u_t = \sum_{n=1}^{\infty} cu_n e^{\alpha t} \cos (n\omega t - \phi_n - \theta_n) \qquad (19)$$

$$W = \bar{W} (1 + W') = \left[1 + \frac{p'}{\gamma}\right]^{1/2} \left[1 + \left(\frac{u_t}{\Delta V}\right)\right]^{1/4} \qquad (20)$$

$$W' = \sum_{n=1}^{\infty} \left(R_n p_n e^{\alpha t} \cos (n\omega t - \phi_n) + I_n p_n e^{\alpha t} \sin (n\omega t - \phi_n)\right) \qquad (21)$$

$$\int_0^{2\pi/\omega} \frac{W'}{e^{\alpha t}} \, dt = 0 \qquad (22)$$

$$R_n + iI_n = \frac{\displaystyle\int_0^{2\pi/\omega} \frac{W'}{e^{\alpha t}} \cos (n\omega t - \phi_n) \, dt}{\displaystyle\int_0^{2\pi/\omega} p_n \cos^2 (n\omega t - \phi_n) \, dt} + i \frac{\displaystyle\int_0^{2\pi/\omega} \frac{W'}{e^{\alpha t}} \sin (n\omega t - \phi_n) \, dt}{\displaystyle\int_0^{2\pi/\omega} p_n \sin^2 (n\omega t - \phi_n) \, dt}$$

$$= (\omega/\pi) \int_0^{2\pi/\omega} \frac{W'}{p_n e^{\alpha t} e^{-i(n\omega t - \phi_n)}} \, dt = (\omega/\pi) \left[\frac{1}{\bar{W}} \int_0^{2\pi/\omega} \frac{W}{p_n e^{i\phi_n} e^{-ik_n t}} \, dt \right.$$

$$\left. - \frac{(1 - e^{-2\alpha/(\omega/\pi)})}{-ik_n p_n e^{i\phi_n}}\right] \qquad (23)$$

$$\overline{W} = \frac{\int_0^{2\pi/\omega} \frac{W}{e^{\alpha t}}\, dt}{\int_0^{2\pi/\omega} \frac{1}{e^{\alpha t}}\, dt} = \frac{\alpha}{\left(1-e^{-2\alpha/(\omega/\pi)}\right)} \int_0^{2\pi/\omega} \frac{W}{e^{\alpha t}}\, dt \qquad (24)$$

Calculations with the revised response factor model did not change the general characteristics of the computed results.

Based on these observations, attempts were made to eliminate the possibility of the looping behavior and to improve the response factor approximation. Calculations were made with a nonzero nozzle admittance in an effort to shift the looping characteristic out of the region of the solution. Results from these calculations which were made for nozzle admittance values that were expected to shift the looping out of the region of interest, are shown in Fig. 11. Some of the characteristics of these results, some baffle lengths lead to greater predicted stability than the zero-length case, appear more nearly compatible with experimentally observed behavior. Nonetheless, peaked characteristic has persisted and the use of a nonzero nozzle admittance is not sufficient to eliminate the undesirable behavior.

In an effort to improve the boundary condition approximation, additional calculations were made for two equally spaced baffles rather than one. This was done to eliminate the pressure node (zero) that gives rise to the singularities exhibited by the harmonic mode response factor curves shown in Fig. 7 through 10. To accomplish these calculations, the computer

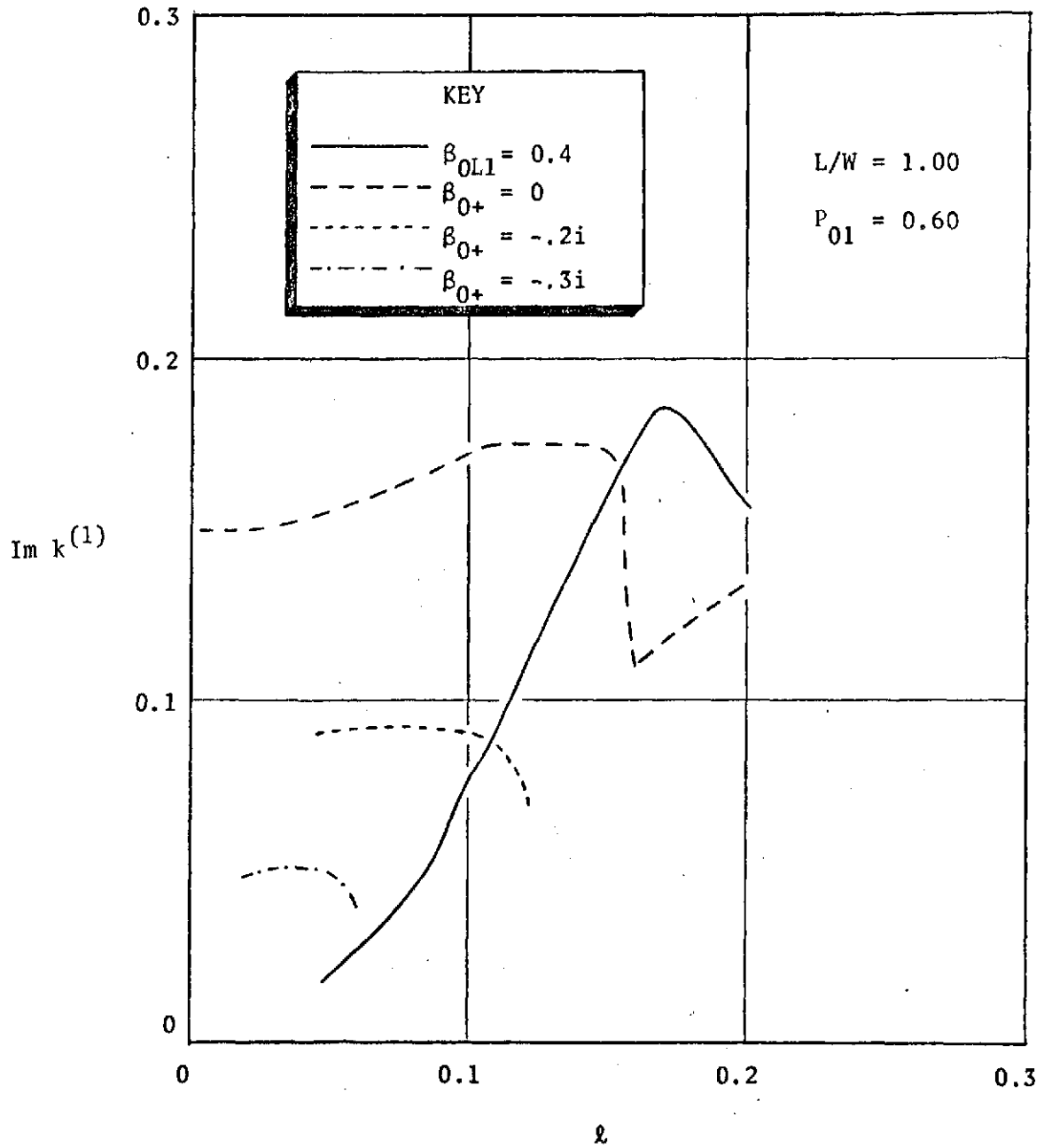

Figure . Variation of Growth Coefficient with Baffle Length for Several Nozzle Admittance Values

program was converted from the Honeywell 440 computer to an IBM-370 TSO computer because the calculations were prohibitively slow on the Honeywell machine (the TSO system was not used originally because it was not available at that time). Calculations were made with both the original and revised versions of the response factor model, with only the latter model being adapted to print out the response factor distribution. Unfortunately, after completion of the effort, a minor programming error was found in the computer subroutine corresponding to the revised response factor model which prevents the use of the results obtained from it. Calculated results obtained with the original response factor model are summarized below (for two baffles, L/W = 1.0, P_{o_1} = 0.1 and $\Delta\overline{V}$ = 0.02):

ℓ	$k^{(1)}$	β_{2L1}	P_{Q2}	ϕ_2/π
0.05	3.569 +0.3496i	-0.737 -0.372i	0.153	-0.0784
0.10	3.366 +0.5705i	-0.611 -0.222i	0.101	0.0077
0.15	2.913 +0.6937i	-0.513 -0.252i	0.100	0.0629
0.20	2.610 +0.6655i	-0.463 -0.273i	0.085	0.0853

These results also show the characteristic increasing growth coefficient (worsening stability) with increasing baffle length until a maximum is reached and then slowly decreasing. Thus, the problem has persisted.

CONCLUDING REMARKS AND RECOMMENDATIONS

It is clear from the foregoing discussion that the computerized model for predicting the effects of baffles on combustion stability, as currently formulated, fails to predict observed stability trends. Clearly, at least some portions of the model inadequately describe important physical phenomena or some important process is omitted. The omitted process may be a nonlinear baffle damping, which was assumed unimportant when the model was originally formulated. However, recent results from bench-scale acoustic model tests at Rocketdyne indicate that this damping is important. Therefore, it may be necessary to incorporate damping into the model to obtain an adequate stability prediction.

The model may also be inadequate in the way in which the combustion is described. Currently, the effects of wave distortion are introduced through use of the second transverse model whereas a nonlinear analysis of the problem may show that the harmonic frequency component should have a much different spatial pressure and velocity distribution. Moreover, the response factor has been coupled through an approximate boundary condition which clearly is inadequate when spatially averaged over the injector face. Additional investigation of the importance of this boundary condition is needed.

The current overall modelling approach cannot be properly evaluated at this point because of the need to allow for a spatially varying boundary condition. Therefore, it is recommended that it be modified to use a separate average injector admittance (or response factor) for each baffle compartment. Although this approximation is less desirable than accounting for the spatial variation completely, it can be accomplished more readily and should be adequate to show the influence of the spatial variation. If the spatial variation is found important, it can be included more fully at a later time.

In addition, the Heidmann response factor analysis indicates a spinning wave is substantially more unstable than a standing wave. Therefore, revision of the model to describe a thin annulus with a spinning mode is recommended.

REFERENCES

1. Oberg, C. L., T. L. Wong, and R. A. Schmeltzer: Analysis of the Acoustic Behavior of Baffled Combustion Chambers, NASA CR-72625, R-8076, Rocketdyne Division, Rockwell International, 6633 Canoga Avenue, Canoga Park, California, January 1970.

2. Oberg, C. L., W. H. Evers, Jr., and T. L. Wong: Analysis of the Wave Motion in Baffled Combustion Chambers, NASA CR-72879, R-8758, Rocketdyne Division, Rockwell International, 6633 Canoga Avenue, Canoga Park, California, October 1971.

3. Heidmann, M., "Amplification by Wave Distortion of the Dynamic Response of Vaporization Limited Combustion," NASA TN D-6287, National Aeronautics and Space Administration, Washington, D. C., May 1971.

4. Morse, P. M. and H. Feshbach: Methods of Theoretical Physics, McGraw-Hill Book Company, Inc., New York, 1953.

5. Morse, P.M. and K. U. Ingard: Theoretical Acoustics, McGraw-Hill Book Company, Inc., New York, 1968.

6. McClure, F. T., R. W. Hart, and R. H. Cantrell: Interaction Between Sound and Flow--Stability of T-Burners, AIAA Journal, Vol I, No. 3, March 1963, pp. 586-590.

7. Cantrell, R. H. and R. W. Hart: Interaction Between Sound and Flow in Acoustic Cavities: Mass, Momentum, and Flow Considerations, Journal Acoust. Soc. Am., Vol. 36, 1964, pp. 697-706.

8. Maslen, S. H. and F. K. Moore: On Strong Transverse Waves Without Shocks in a Circular Cylinder, Journal of Aeronautical Sciences, June 1956, pp. 583-593.